



Cite this: *Chem. Sci.*, 2022, **13**, 1946

All publication charges for this article have been paid for by the Royal Society of Chemistry

Received 3rd December 2021  
Accepted 14th January 2022

DOI: 10.1039/d1sc06760e

[rsc.li/chemical-science](http://rsc.li/chemical-science)

## Introduction

Rearrangements have been fascinating topics to organic chemists due to their innate charm and versatile use in skeleton reconstruction.<sup>1,2</sup> The classic ionic-type named reactions, such as Pinacol, Favorskii, Beckmann, Claisen and Smiles rearrangements, involve the re-organization of certain carbon skeletons.<sup>3–6</sup> In contrast, the examples for heteroatom shifts are relatively rare. For example, the Brook rearrangement<sup>7,8</sup> and Doyle–Kirmse reactions<sup>9–12</sup> involve silyl and thiol group migrations. A series of 1,2-boryl migrations of  $\alpha$ -boryl epoxides and carboxylic acids have been reported by Yudin and co-workers.<sup>13,14</sup> Besides the ionic type functional group migrations (FGM), the rearrangements that involve free radicals have demonstrated versatile reactivities towards remote FGM for the construction of more complex molecular frameworks.<sup>15–19</sup> Recent progress on aryl, cyano, alkynyl, and carbonyl group migration protocols have been well-documented for the construction of new C–C bonds *via* radical pathways.<sup>1,20–32</sup> Boron shift chemistry, which represents tremendous importance for the broad utility of boronic acids and esters, has attracted much attention of organic chemists. The first example of radical type boron shift was reported by Batey and Smil.<sup>33</sup> In 2019, Aggarwal described a radical 1,2-boron shift of diboronates under photocatalysis to access 1,2-difunctionalized boronates (Fig. 1A).<sup>34</sup> Studer and co-workers applied the boron migration protocol to 1,3-difunctionalized trifluoromethylated alkynyl boronates (Fig. 1B).<sup>35</sup> In contrast, the analogous 1,3-shift process has encountered inevitable difficulties because of the disfavored

State Key Laboratory of Coordination Chemistry, Jiangsu Key Laboratory of Advanced Organic Materials, School of Chemistry and Chemical Engineering, Nanjing University, Nanjing 210023, China. E-mail: [yiwang@nju.edu.cn](mailto:yiwang@nju.edu.cn)

† Electronic supplementary information (ESI) available. CCDC 2115384. For ESI and crystallographic data in CIF or other electronic format see DOI: [10.1039/d1sc06760e](https://doi.org/10.1039/d1sc06760e)

## Radical boron migration of allylboronic esters†

Xiangzhang Tao, Shengyang Ni, Lingyu Kong, Yi Wang \* and Yi Pan

A photocatalyzed 1,3-boron shift of allylboronic esters is reported. The boron atom migration through the allylic carbon skeleton proceeds *via* consecutive 1,2-boron migrations and Smiles-type rearrangement to furnish a variety of terminally functionalized alkyl boronates. Several types of migrating variations of heteronuclei radicals and dearomatization processes are also tolerated, allowing for further elaboration of highly functionalized boron-containing frameworks.

four-membered cyclic transition state and no example of  $\gamma$ -boron migration has been reported.<sup>36–42</sup> Theoretical studies on such 1,3-boron migrating processes have been concluded to be thermodynamically unfavorable and experimentally inaccessible.<sup>43</sup> We envisioned that through consecutive boron migration on the carbon skeleton, the boronic ester moiety could switch to the remote end of the allylic backbones for the formation of more stable radical intermediates. Herein, we described a radical 1,3-boron migration process merging double 1,2-boron shifts of allylboronates and Smiles-type rearrangement of arylsulfonyl radicals to generate aryl  $\gamma$ -boronates (Fig. 1C). Moreover, this boron migration protocol could be further extended to other heteronuclei radicals and the formation of dearomatized frameworks.

## Results and discussion

Our investigations began with the model reaction of sodium arylsulfonate **1a** and allylboronic ester **2a**. The desired 1,3-

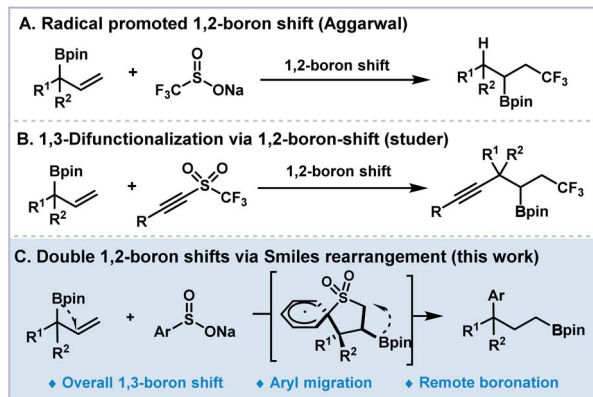


Fig. 1 Radical promoted boron shift chemistry.



Table 1 Optimization of the reaction conditions<sup>a</sup>

Entry	Variation from the above conditions	Yield of 3a <sup>b</sup>
1	None	95 (82%) <sup>c</sup>
2	Ir(ppy) <sub>3</sub> instead of PTH	20
3	4CzIPN instead of PTH	35
4	Acr <sup>+</sup> ClO <sub>4</sub> <sup>-</sup> instead of PTH	85
5	DMF instead of CHCl <sub>3</sub>	0
6	MeOH instead of CHCl <sub>3</sub>	0
7	w/o HOAc	58
8	w/o PTH	0
9	In darkness	0

<sup>a</sup> Reaction conditions: 1a (0.3 mmol), 2a (0.2 mmol), 10-phenylphenothiazine (PTH, 8 mol%), HOAc (4.0 equiv.), CHCl<sub>3</sub> (2 mL), Ar, irradiation with 60 W blue LEDs at r.t. for 12 h. <sup>b</sup> Crude yields were determined by <sup>19</sup>F NMR using 1,4-difluorobenzene as the internal standard. <sup>c</sup> The isolated yields were determined from the corresponding oxidized product.

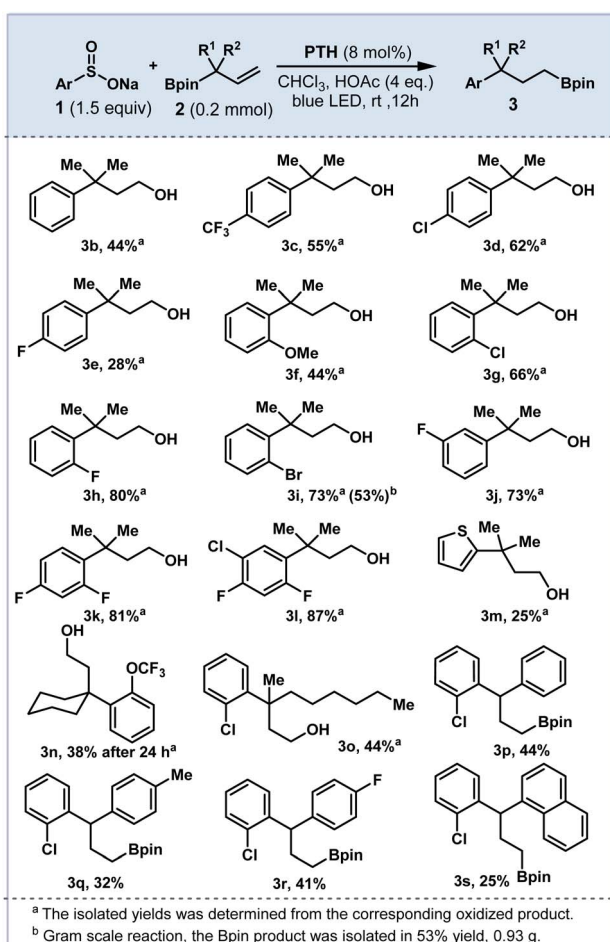


Fig. 2 Scope of the 1,3-boron shift.

boron migration product 3a could be obtained in 95% yield under blue LED irradiation for 12 h with 10-phenylphenothiazine (PTH) as the photocatalyst and acetic acid as the additive in CHCl<sub>3</sub> (entry 1). For other photocatalysts such as Ir(ppy)<sub>3</sub> and 4CzIPN, lower yields were noted (20–35%, entries 2 and 3). Replacing the PTH photocatalyst with Acr<sup>+</sup>ClO<sub>4</sub><sup>-</sup> led to a slightly lower yield (entry 4). The reaction could not occur in DMF or MeOH (entry 5 and 6). In the absence of acetic acid, the reaction yield was reduced significantly (entry 7). Control experiments indicated that light and the photocatalyst are necessary for this boron shift strategy (entries 8 and 9, see the ES<sup>†</sup>) (Table 1).

With the optimized reaction conditions in hand, we explored the generality of the protocol with various sodium arylsulfonates and allylboronic esters (Fig. 2). Arylsulfonates bearing either electron-withdrawing or electron-donating groups delivered the desired 1,3-boron shift products in moderate to good yields (3b–3l, 25–87%). The *ortho*-fluorinated arylsulfonate provided the product 3h in 80% yield, while the migration of *para*- and *meta*-fluorinated substrates was less efficient (30% for 3e and 27% for 3j). Multiple fluorine or chlorine substituted arylsulfonates could be tolerated (3k and 3l). Heteroarene 3m was compatible with the reaction conditions, and the low yield was due to the electronic effect of thiophene. Allylboronates with various substitutions were also investigated. For example, substrates bearing the cyclohexyl group gave the boronation product with a lower efficiency (3n, 38%). The arylboronate 3o with unsymmetrical alkyl substituents was afforded in 44% yield (R<sup>1</sup> = Me, R<sup>2</sup> = n-Hex). Furthermore, this boron shift was proven successful with stabilized benzyl radical precursors (R<sup>1</sup> = Ar, R<sup>2</sup> = H). Aryl substituted allylboronates have been subjected to the standard conditions and diarylpropylboronic products were readily accessed. The  $\alpha$ -phenyl-substituted allylboronic esters containing phenyl, *para*-methyl and *para*-fluorine phenyl and naphthyl could deliver the corresponding products (3p–3s). The low yields of 3e, 3n and 3q were due to the loss in the purification process.

Photoredox-catalyzed and electrochemical dearomatization processes involving radicals have been explored with proven utility.<sup>44–50</sup> During the investigation of this 5-*exo*-trig cyclization process, we also observed the 6-*exo*-trig cyclization dearomatized products in the reaction mixture.<sup>51–53</sup> As valuable pharmacophores, cyclic sulfones have been widely applied in medicinal chemistry and organic photoconducting materials due to their unique electronic and optical properties.<sup>54–56</sup> With a slight variation of the reaction conditions (eosin Y and DMF), the dearomatized product 4 could be readily afforded *via* 1,2-boron shift and radical addition. As shown in Fig. 3, tetrohydrothiochromene sulfone 4a was achieved in 82% yield with excellent diastereoselectivity (>20 : 1, the absolute configuration was confirmed by XRD analysis). Similarly, electron-withdrawing group substituted 4b–4e were obtained in 47–86% yields. In the cases of 4d and 4e, small amounts of the protonated by-products were observed. Interestingly, 3-fluoro and 3,4-difluoro substituted arylsulfonate substrates generated single dearomatized regioisomers in good yields (4f and 4g), which was governed by the regio- and chemoselective



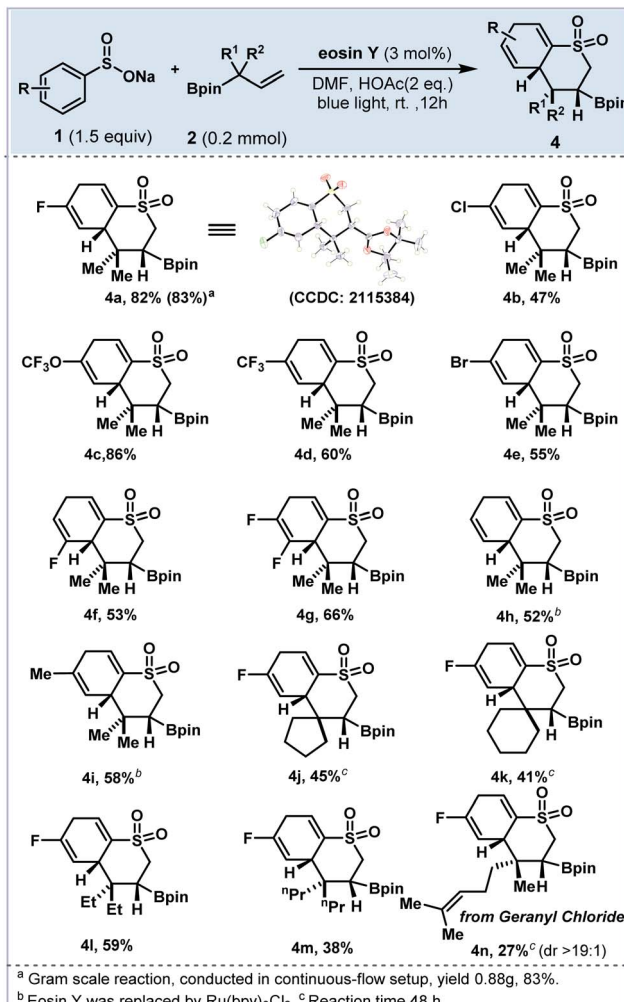


Fig. 3 Substrate scope of dearomatized products.

nature of the cyclization step. Notably, dearomatized products **4h** and **4i** were furnished along with the corresponding aromatized cyclic sulfones. Replacing the photocatalyst with Ru(bpy)<sub>3</sub>Cl<sub>2</sub>, the aromatic by-products were significantly suppressed (De/Ar = 10 : 1 for **4i** and >20 : 1 for **4h**). Next, different allylboronic esters were explored with sodium arylsulfonate **1a** under this protocol (**4j**–**4n**). Substrates bearing five- and six-membered rings also afforded the corresponding products **4j** and **4k** in moderate yields (41–47%). The 2,2-diethyl and 2,2-dipropyl alkenyl boronic esters delivered the dearomatized products **4l** and **4m** in 59% and 38% yields, respectively. The allylboronate derived from geranyl chloride gave **4n** in 27% yield as a single diastereoisomer (d.r. > 19 : 1).

In order to better understand the reaction pathway, we have added a catalytic amount of thiophenol to quench the tertiary C-radical generated by 1,2-boron migration of the allylboronates (Fig. 4). A diverse set of aromatic substrates, regardless of their electronic properties were found to be compatible to produce the corresponding 1,2-difunctionalized products (**5a**–**e**). Allylboronate containing a quaternary carbon center provided the

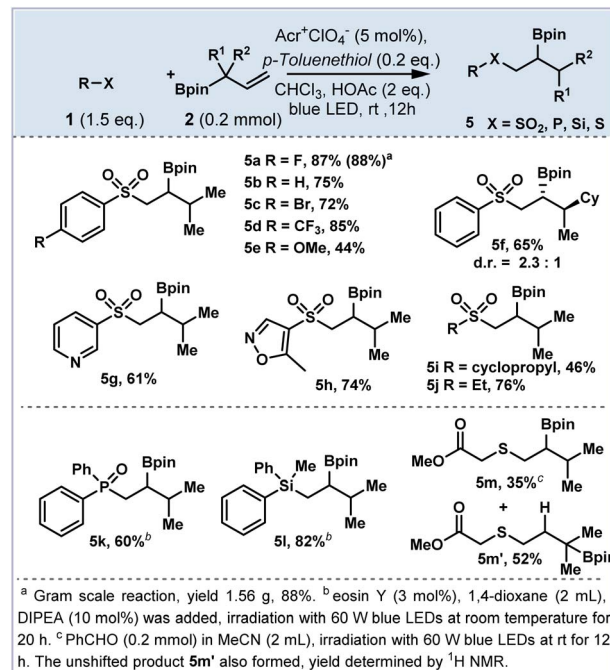


Fig. 4 Scope of 1,2-boron shift.

corresponding product **5f** with a diastereomeric ratio of 2.3 : 1. The heteroaryl sulfones bearing pyridine (**5g**) and oxazole (**5h**) could be tolerated. The alkyl sulfonates (**5i** and **5j**) were also furnished in good yields. Moreover, other heteroatom radical precursors could be tolerated to construct C-P, C-Si and C-S bonds. For example, phosphate and diphenylmethylsilane delivered  $\beta$ -boronate products **5k** and **5l** in 60% and 82% yields, respectively. The mercaptan derivative afforded the thiolated boronate **5m** in 35% yield in the mixture with the unshifted product **5m'**.

Based on the above results, a plausible mechanism was proposed (Fig. 5). First, the photocatalysts were activated to their excited state by blue light and they underwent single electron transfer (SET) with arylsulfonate to produce sulfone radical **int I**. The conjugate addition of **int I** to allylboronate **2** produced the secondary carbon radical **int II** and 1,2-boron shift generated the tertiary carbon radical **int III**. At this point, the radical **int III** could undergo different pathways depending on the conditions. Under condition A, 5-exo-trig cyclization followed by Smiles-type rearrangement afforded **int IV** which degraded to release SO<sub>2</sub> and the second 1,2-boron shift provided the  $\beta$ -carbon radical **int V**. Next, the hydrogen atom transfer (HAT) process occurred between radical **int V** and CHCl<sub>3</sub> to deliver the 1,3-boron shift products **3** and  $^3$ CCl<sub>3</sub> (see deuteration experiments in the ESI† for details). Finally, the trichloromethyl radical underwent SET with PC<sup>·</sup> to close the photoredox catalysis cycle. However under condition B, the tertiary radical **int III** could undergo 6-exo-trig cyclization to deliver the dearomatized product **4**. Under condition C, the radical **int III** underwent HAT with thiophenol to form the 1,2-difunctionalized product **5**.

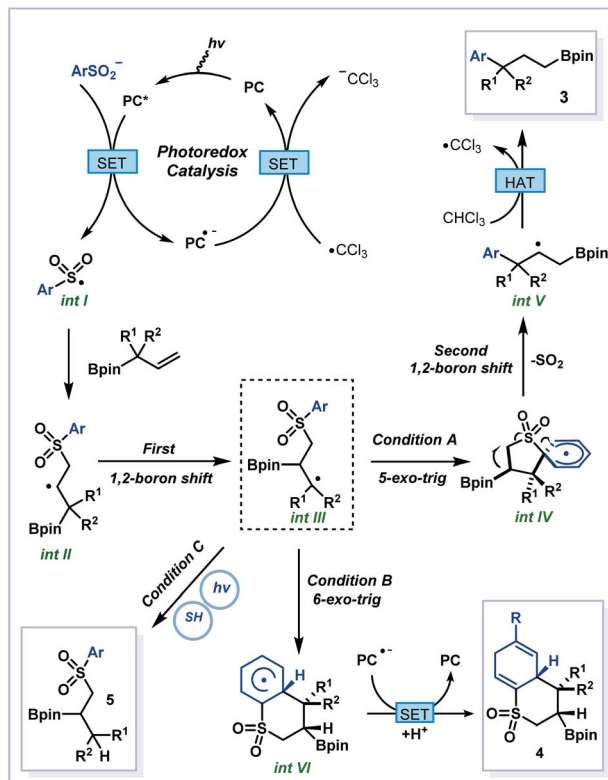


Fig. 5 Plausible mechanism for 1,3- and 1,2-boron migrations.

## Experimental

### General procedure for product 3 formation (condition A)

Under argon, PTH (8 mol%) and sodium benzenesulfinate **1** (0.3 mmol, 1.5 equiv.) were placed in a tube with a stirring bar, and then  $\text{CHCl}_3$  (2 mL) was added at room temperature. Subsequently, the corresponding allylboronic acid pinacol ester (0.2 mmol, 1.0 equiv.) and HOAc (0.8 mmol, 4.0 equiv.) were added dropwise *via* syringe. After that, the tube was exposed to 60 W blue LEDs at room temperature for about 12 h. The mixture was concentrated *in vacuo*. Then it was passed through a short pad of silica gel. The organic layer was concentrated under vacuum and the yellow oily residue was diluted with THF (1 mL) and water (1 mL) followed by addition of  $\text{NaBO}_3 \cdot 4\text{H}_2\text{O}$  (61.5 mg, 0.4 mmol). The mixture was allowed to stir for 3 h at rt. The reaction mixture was washed with EtOAc (5 mL  $\times$  3) and the combined organic layers were dried over  $\text{MgSO}_4$ . It was then concentrated and purified by silica gel chromatography to afford the desired product.

### General procedure for product 4 formation (condition B)

Under argon, Eosin Y (3 mol%) and sodium benzenesulfinate **1** (0.3 mmol, 1.5 equiv.) were placed in a tube with a stirring bar, and then  $\text{CHCl}_3$  (2 mL) was added at room temperature. Subsequently, the corresponding allylboronic acid pinacol ester (0.2 mmol, 1.0 equiv.) and HOAc (0.4 mmol, 2.0 equiv.) were added dropwise *via* syringe. After that, the tube was exposed to 60 W blue LEDs at room temperature for about 12–24 h. Upon

completion, the solution was passed through a pad of silica gel and washed with ethyl acetate. The filtrate was concentrated under vacuum and purified by column chromatography on silica gel using 10 : 1–5 : 1 hexane : EtOAc as the eluent to give the corresponding pure product **4**.

### General procedure for product 5 formation (condition C)

Under argon,  $\text{Acr}^+\text{ClO}_4^-$  (5 mol%), sodium benzenesulfinate **1** (0.3 mmol, 1.5 equiv.) and *p*-toluenethiol (0.04 mmol, 0.2 equiv.) were placed in a tube with a stirring bar, and then  $\text{CHCl}_3$  (2 mL) was added at room temperature. Subsequently, the corresponding allylboronic acid pinacol ester (0.2 mmol, 1.0 equiv.) and HOAc (0.4 mmol, 2.0 equiv.) were added dropwise *via* syringe. After that, the tube was exposed to 60 W blue LEDs at room temperature for about 12 h. The mixture was concentrated and purified by silica gel chromatography to afford the desired product **5**.

## Conclusions

In conclusion, a photocatalytic 1,3-boron shift protocol merging radical migration and Smiles-type rearrangement is developed. The atom switch acrobatics undergoes consecutive secondary/tertiary and primary/secondary carbon radical migrations to access a variety of 1,3-difunctionalized aryl boronates. The variation of the conditions could also lead to other 1,2-boron shift products including phosphate, silyl and thiol derivatives and dearomatized sulfone-fused ring systems. This boron migration strategy has provided a new pathway for remote functional group migration. Further studies of boron shift chemistry are underway in the laboratory.

## Data availability

The data that support the findings of this study are available in the ESI† or on request from the corresponding author.

## Author contributions

X. T. conducted all experiments and characterized the novel compounds. S. N., L. K., Y. W. and Y. P. designed the experiments and wrote the manuscript.

## Conflicts of interest

The authors declare no competing interests.

## Acknowledgements

We gratefully acknowledge the financial support from the National Natural Science Foundation of China (No. 21772085, 21971107 and 22071101).

## Notes and references

- X. Wu and C. Zhu, *Acc. Chem. Res.*, 2020, **53**, 1620–1636.
- C. M. Rojas, *Molecular Rearrangements in Organic Synthesis*, Wiley-VCH, New York, 2015.



3 M. Kischkowitz, F. W. Friese and A. Studer, *Adv. Synth. Catal.*, 2020, **362**, 2077–2087.

4 D. Leonori and V. K. Aggarwal, *Acc. Chem. Res.*, 2014, **47**, 3174–3183.

5 W. Li, W. Xu, J. Xie, S. Yu and C. Zhu, *Chem. Soc. Rev.*, 2018, **47**, 654–667.

6 S. Namirembe and J. P. Morken, *Chem. Soc. Rev.*, 2019, **48**, 3464–3474.

7 A. G. Brook, *J. Am. Chem. Soc.*, 1958, **80**, 1886–1889.

8 A. G. Brook, C. M. Warner and M. E. McGriskin, *J. Am. Chem. Soc.*, 1959, **81**, 981–984.

9 W. Kirmse and M. Kapps, *Chem. Ber.*, 1968, **101**, 994–1003.

10 X. Lin, Y. Tang, W. Yang, F. Tan, L. Lin, X. Liu and X. Feng, *J. Am. Chem. Soc.*, 2018, **140**, 3299–3305.

11 M. P. Doyle, W. H. Tamblyn and V. Bagheri, *J. Org. Chem.*, 1981, **46**, 5094–5102.

12 Z. Zhang, Z. Sheng, W. Yu, G. Wu, R. Zhang, W. D. Chu, Y. Zhang and J. Wang, *Nat. Chem.*, 2017, **9**, 970–976.

13 Z. He, A. Zajdlik, J. D. St Denis, N. Assem and A. K. Yudin, *J. Am. Chem. Soc.*, 2012, **134**, 9926–9929.

14 C. F. Lee, D. B. Diaz, A. Holownia, S. J. Kaldas, S. K. Liew, G. E. Garrett, T. Dudding and A. K. Yudin, *Nat. Chem.*, 2018, **10**, 1062–1070.

15 Z. Li, M. Wang and Z. Shi, *Angew. Chem., Int. Ed.*, 2021, **60**, 186–190.

16 A. A. Tabolin and S. L. Ioffe, *Chem. Rev.*, 2014, **114**, 5426–5476.

17 T. H. West, S. S. M. Spoehrle, K. Kasten, J. E. Taylor and A. D. Smith, *ACS Catal.*, 2015, **5**, 7446–7479.

18 J. J. Zhang, L. Yang, F. Liu, Y. Fu, J. Liu, A. A. Popov, J. Ma and X. Feng, *Angew. Chem., Int. Ed.*, 2021, **60**, 25695–25700.

19 Y. Zhu, L. Sun, P. Lu and Y. Wang, *ACS Catal.*, 2014, **4**, 1911–1925.

20 W. H. Urry and M. S. Kharasch, *J. Am. Chem. Soc.*, 1944, **66**, 1438–1440.

21 N. Fuentes, W. Kong, L. Fernandez-Sanchez, E. Merino and C. Nevado, *J. Am. Chem. Soc.*, 2015, **137**, 964–973.

22 W. Kong, M. Casimiro, N. Fuentes, E. Merino and C. Nevado, *Angew. Chem., Int. Ed.*, 2013, **52**, 13086–13090.

23 W. Kong, E. Merino and C. Nevado, *Angew. Chem., Int. Ed.*, 2014, **53**, 5078–5082.

24 C. Hervieu, M. S. Kirillova, T. Suarez, M. Muller, E. Merino and C. Nevado, *Nat. Chem.*, 2021, **13**, 327–334.

25 W. Kong, N. Fuentes, A. Garcia-Dominguez, E. Merino and C. Nevado, *Angew. Chem., Int. Ed.*, 2015, **54**, 2487–2491.

26 W. Kong, M. Casimiro, E. Merino and C. Nevado, *J. Am. Chem. Soc.*, 2013, **135**, 14480–14483.

27 J. J. Douglas, H. Albright, M. J. Sevrin, K. P. Cole and C. R. Stephenson, *Angew. Chem., Int. Ed.*, 2015, **54**, 14898–14902.

28 D. Alpers, K. P. Cole and C. R. J. Stephenson, *Angew. Chem., Int. Ed.*, 2018, **57**, 12167–12170.

29 Y. Xia and A. Studer, *Angew. Chem., Int. Ed.*, 2019, **58**, 9836–9840.

30 N. Radhoff and A. Studer, *Angew. Chem., Int. Ed.*, 2021, **60**, 3561–3565.

31 Y. Xia, L. Wang and A. Studer, *Angew. Chem., Int. Ed.*, 2018, **57**, 12940–12944.

32 F. W. Friese, C. Mück-Lichtenfeld and A. Studer, *Nat. Commun.*, 2018, **9**, 2808.

33 R. A. Batey and D. V. Smil, *Angew. Chem., Int. Ed.*, 1999, **38**, 1798–1800.

34 D. Kaiser, A. Noble, V. Fasano and V. K. Aggarwal, *J. Am. Chem. Soc.*, 2019, **141**, 14104–14109.

35 K. Jana, A. Bhunia and A. Studer, *Chem.*, 2020, **6**, 512–522.

36 Y. Ishida, I. Nakamura and M. Terada, *J. Am. Chem. Soc.*, 2018, **140**, 8629–8633.

37 Y. Chen, Y. Liu, Z. Li, S. Dong, X. Liu and X. Feng, *Angew. Chem., Int. Ed.*, 2020, **59**, 8052–8056.

38 M. N. Alam, S. R. Dash, A. Mukherjee, S. Pandole, U. K. Marelli, K. Vanka and P. Maity, *Org. Lett.*, 2021, **23**, 890–895.

39 I. Nakamura and M. Terada, *Tetrahedron Lett.*, 2019, **60**, 689–698.

40 K. Włodarczyk, P. Borowski and M. Stankevič, *Beilstein J. Org. Chem.*, 2020, **16**, 88–105.

41 M. E. Gurskii, P. A. Belyakov, K. A. Lyssenko, A. L. Semenova and Y. N. Bubnov, *Russ. Chem. Bull.*, 2014, **63**, 480–486.

42 D. Wang, K. Jana and A. Studer, *Org. Lett.*, 2021, **23**, 5876–5879.

43 D. Wang, C. Muck-Lichtenfeld and A. Studer, *J. Am. Chem. Soc.*, 2020, **142**, 9119–9123.

44 B. K. Peters, K. X. Rodriguez, S. H. Reisberg, S. B. Beil, D. P. Hickey, Y. Kawamata, M. Collins, J. Starr, L. Chen, S. Udyavara, K. Klunder, T. J. Gorey, S. L. Anderson, M. Neurock, S. D. Minteer and P. S. Baran, *Science*, 2019, **363**, 838–845.

45 A. Chatterjee and B. Konig, *Angew. Chem., Int. Ed.*, 2019, **58**, 14289–14294.

46 Y. Z. Cheng, X. L. Huang, W. H. Zhuang, Q. R. Zhao, X. Zhang, T. S. Mei and S. L. You, *Angew. Chem., Int. Ed.*, 2020, **59**, 18062–18067.

47 Y. Z. Cheng, Q. R. Zhao, X. Zhang and S. L. You, *Angew. Chem., Int. Ed.*, 2019, **58**, 18069–18074.

48 A. R. Flynn, K. A. McDaniel, M. E. Hughes, D. B. Vogt and N. T. Jui, *J. Am. Chem. Soc.*, 2020, **142**, 9163–9168.

49 M. J. James, J. L. Schwarz, F. Strieth-Kalthoff, B. Wibbeling and F. Glorius, *J. Am. Chem. Soc.*, 2018, **140**, 8624–8628.

50 E. H. Southgate, J. Pospech, J. Fu, D. R. Holycross and D. Sarlah, *Nat. Chem.*, 2016, **8**, 922–928.

51 T. M. Monos, R. C. McAtee and C. R. J. Stephenson, *Science*, 2018, **361**, 1369–1373.

52 J. Shi, L. Li, C. Shan, Z. Chen, L. Dai, M. Tan, Y. Lan and Y. Li, *J. Am. Chem. Soc.*, 2021, **143**, 10530–10536.

53 R. C. McAtee, E. A. Noten and C. R. J. Stephenson, *Nat. Commun.*, 2020, **11**, 2528.

54 M. E. Cinar and T. Ozturk, *Chem. Rev.*, 2015, **115**, 3036–3140.

55 L. Duan, J. Qiao, Y. Sun and Y. Qiu, *Adv. Mater.*, 2011, **23**, 1137–1144.

56 F. Velazquez, M. Sannigrahi, F. Bennett, R. G. Lovey, A. Arasappan, S. Bogen, L. Nair, S. Venkatraman, M. Blackman, S. Hendrata, Y. Huang, R. Huelgas, P. Pinto, K. C. Cheng, X. Tong, A. T. McPhail and F. G. Njoroge, *J. Med. Chem.*, 2010, **53**, 3075–3085.

